Increased fibrillar amyloid-β burden in normal individuals with a family history of late-onset Alzheimer's

Lisa Mosconi[a,1], Juha O. Rinne[b], Wai H. Tsui[a,c], Valentina Berti[a,d], Yi Li[a], Huiyu Wang[a], John Murray[a], Noora Scheinin[b], Kjell Någren[b,e], Schantel Williams[a], Lidia Glodzik[a], Susan De Santi[a], Shankar Vallabhajosula[f], and Mony J. de Leon[a,c,1]

[a]New York University School of Medicine, New York, NY 10016; [b]Turku PET Centre, University of Turku, Turku FIN 20520, Finland; [c]Nathan Kline Institute, Orangeburg, NY 10962; [d]University of Florence, Florence 50134, Italy; [e]PET and Cyclotron Unit, Odense University Hospital, Odense DK-5000, Denmark; and [f]Weill Cornell Medical College, New York, NY 10021

Having a parent affected with late-onset Alzheimer's disease (LOAD) is a major risk factor among cognitively normal (NL) individuals. This ^{11}C-Pittsburgh Compound B (PiB)-PET study examines whether NL individuals with LOAD parents show increased fibrillar amyloid-beta (Aβ) deposition, a hallmark of Alzheimer's disease (AD) pathology and whether there are parent-of-origin effects. Forty-two 50- to 80-year-old NL persons were examined with PiB-PET. These individuals included 14 NL subjects with a maternal family history (FH) of LOAD (FHm), 14 NL subjects with a paternal FH (FHp), and 14 NL subjects with a negative family history of any dementia (FH−). Statistical parametric mapping and automated regions-of-interest were used to compare cerebral-to-cerebellar PiB standardized uptake value ratios, reflecting fibrillar Aβ burden, across groups. FH groups did not differ in age, gender, education, and apolipoprotein E (ApoE) status. NL FHm subjects showed higher PiB retention in AD-affected anterior and posterior cingulate cortex (PCC), precuneus, parietal, temporal, occipital, and frontal cortices, right basal ganglia, and thalamus, compared with FH− and FHp subjects. FHp subjects showed increased PiB retention in the PCC and frontal cortex, intermediate between FHm and FH− subjects. Results remained significant after controlling for age, gender, education, and ApoE status. Children of parents with LOAD, particularly those with affected mothers, have increased fibrillar Aβ load in AD-vulnerable regions compared with controls, perhaps accounting for the known increased risk for AD. Present findings may motivate further research on familial transmission and parent-of-origin effects in LOAD.

early detection | PET imaging | presymptomatic

Alzheimer's disease (AD) is a neurodegenerative disease characterized by insidious onset and progressive cognitive impairment. This course makes the initial stages of AD difficult to distinguish from normal aging. To develop prevention treatments for AD, it is necessary to identify persons who are cognitively intact but have high risk for developing the disease. Such individuals are most likely to benefit from therapies instituted before irreversible neuronal injury, when the potential for preservation of function is the greatest.

Rare genetic mutations have been identified among the early-onset forms of AD (EOAD), but the genetics of the more common late-onset AD (LOAD) remain elusive (1). Although some LOAD cases appear to be sporadic in nature, genetically mediated risk is evident from the familial aggregation of many LOAD cases. After advanced age, having a first-degree family history of LOAD, especially when a parent is affected, is the most significant risk factor for developing AD (2, 3).

Studies of EOAD indicate that amyloid-beta (Aβ) dysmetabolism may be a primary event in the pathogenesis of AD (1). Fibrillar Aβ deposition in senile plaques is a cardinal neuropathological feature in AD and develops many years before the clinical manifestations of disease become evident (4, 5). However, it is unclear whether increased Aβ deposition is also an early initiating event in LOAD (1).

PET tracers with high affinity for the aggregated forms of Aβ found in senile plaques have been developed to image brain Aβ deposits in vivo. The best-characterized Aβ tracer is Pittsburgh Compound B (PiB) (6). Consistent with postmortem studies, high PiB retention in amyloid-rich regions is observed consistently in AD patients, in many patients with mild cognitive impairment, and in up to 30% of cognitively normal (NL) elderly persons (6–9). It is not known whether Aβ deposition is increased in NL individuals with a first-degree family history of LOAD.

This study examines whether NL individuals with LOAD-affected parents show increased Aβ load compared with NL individuals with no family history of AD. Moreover, in light of recent results that NL individuals with affected mothers (FHm) show more severe brain hypometabolism (10, 11) and atrophy (12) than those with affected fathers (FHp), we examined whether there are parent-of-origin effects on Aβ burden.

Results

Demographic characteristics of the subjects under study are shown in Table 1. There were no differences between groups in age, gender distribution, education, apolipoprotein E (ApoE) status, and Mini-Mental Status Examination (MMSE) scores. On regions-of-interest (ROI) analysis, significant differences between groups with a family history (FH) negative for AD (FH−) and groups with a positive family history for AD (FH+) were found in the medial frontal gyrus (MFG), posterior cingulate (PCC), the prefrontal cortex (PFC), and occipital cortex (OCC), inferior parietal (IPL) and lateral temporal lobes (LTL) bilaterally, in the anterior putamen (AntPut) and thalamus of the right hemisphere, and in a composite cortical ROI (AD-mask) ($P < 0.05$) (Table 1). On posthoc examination of FH+ subgroups, the results were driven by the FHm group, which showed higher PiB retention in all these ROIs compared with the FH− group, and higher PiB in the IPL, LTL, and OCC bilaterally, in the right AntPut and thalamus, and in the right MFG and PFC compared with the FHp group (Table 1). The FHp group showed a trend toward higher PiB retention in the PCC and left MFG as compared with the FH− group ($P \geq 0.08$). In these ROIs, there was a significant association between FH status and PiB retention, resulting in an order effect such that PiB binding was higher in FHm > FHp > FH− ($R^2 \geq 0.33$,

MEDICAL SCIENCES

Table 1. Clinical and ^{11}C-PiB ROI measures by family history groups

		FH+		Pairwise *P* values*		
ROI CMRglc	FH−	FHp	FHm	FH− vs. FHp	FH− vs. FHm	FHp vs. FHm
N	14	14	14			
Age (years)	67(7)	66(7)	64(7)			
Gender (females/males)	5/9	7/7	7/7			
Education (years)	10(4)	11(4)	11(5)			
ApoE ε4 ($^{+/−}$) [ε3/ε4, ε4/ε4]	4/10 [4, 0]	7/7 [5, 2]	7/7 [6, 1]			
MMSE	28.6(1.1)	28.7 (1.4)	28.6 (1.5)			
PiB SUVR measures (unitless)						
Anterior putamen						
Left	1.41 (0.17)	1.50 (0.24)	1.65 (0.49)		[0.07]	
Right	1.45 (0.19)	1.51 (0.23)	1.74 (0.49)		0.02	0.05
Inferior parietal lobe						
Left	1.34(0.19)	1.45 (0.21)	1.64(0.33)		0.005	0.05
Right	1.19 (0.15)	1.29 (0.20)	1.47 (0.25)		0.007	0.05
Lateral temporal lobe						
Left	1.31 (0.15)	1.37 (0.20)	1.56 (0.26)		0.007	0.03
Right	1.27 (0.16)	1.30 (0.23)	1.53 (0.33)		0.006	0.05
Medial frontal gyrus						
Left	1.26(0.14)	1.35 (0.29)	1.58 (0.45)	[0.08]	0.006	[0.07]
Right	1.09 (0.13)	1.19 (0.17)	1.37 (0.40)		0.008	0.04
Occipital cortex						
Left	1.32 (0.17)	1.36 (0.15)	1.51 (0.16)		0.01	0.05
Right	1.29(0.17)	1.33 (0.14)	1.47 (0.17)		0.008	0.03
Posterior cingulate cortex						
Left	1.29 (0.15)	1.47 (0.26)	1.68 (0.40)	[0.09]	0.02	
Right	1.34 (1723)	1.50 (0.28)	1.58 (0.46)	[0.09]	0.008	
Prefrontal cortex						
Left	1.22 (0.14)	1.34 (0.22)	1.54 (0.42)		0.004	
Right	1.20 (0.15)	1.34 (0.18)	1.52 (0.38)		0.009	0.05
Thalamus						
Left	1.50 (0.45)	1.46 (0.40)	1.52 (0.35)			
Right	1.39 (0.19)	1.40 (0.21)	1.60 (0.26)		0.03	0.03
AD mask	1.50 (0.21)	1.55 (0.27)	1.80 (0.29)		0.008	0.02

Values are mean (SD), range. ^{11}C-PiB SUVR are cerebral-to-cerebellar gray matter.
*$P < 0.05$. Linear trends are in brackets.

$F \geq_{[1,40]}$ 4.76, $P < 0.04$). No ROIs showed increased PiB retention in the FH− and FHp groups compared with the FHm group.

All results remained significant after controlling for age, gender, education, and ApoE status (Fig. 1). Overall, PiB retention was highest in FHm group and lowest in FH− group in all ROIs. FHp subjects were intermediate between FHm and FH− subjects in PCC and MFG and were comparable to FH− subjects in other ROIs.

Examination of the PiB-PET scans of the offspring of post-mortem-verified AD parents showed that, as compared with controls, the two NL offspring of AD-confirmed fathers showed Z scores within norms, whereas both NL offspring of AD-confirmed mothers had Z scores ≥ 1.5 in most ROIs. Specifically, a 70-year-old FHm man had a Z score ≥ 2.5 in all ROIs, and a 77-year-old FHm woman had a Z score ≥ 1.5 in cortical ROIs but not in the thalamus and AntPut (Fig. S1).

Within the group of ApoE ε4 carriers, the FHm group had higher PiB retention in the regions mentioned above than did the FH− group and higher PiB retention in the bilateral IPL, LTL, OCC, left MFG, and AD-mask than did the FHp group (Mann–Whitney $P \leq$ 0.05). The FHp group showed increased PiB in the bilateral PFC, left MFG, and PCC and nonsignificant trends for the right PCC and MFG compared with the FH− group (Mann–Whitney $P \leq 0.01$).

On statistical parametric mapping (SPM) analysis, significant differences between the FH− and FH+ groups were found in the MFG, PFC, inferior frontal gyrus (IFG), PCC/precuneus, anterior cingulate cortex (ACC), temporal, parietal, and occipital cortex, and fusiform gyri bilaterally, and in basal ganglia and thalamus of the right hemisphere ($P < 0.001$, uncorrected) (Fig. S2). On posthoc examination, the FHm group showed higher PiB retention in all the above brain regions as compared with the FH− group and higher PiB retention in the bilateral PCC/precuneus, IPL, PFC, ACC, and in the left temporal, OCC, MFG, and IFG as compared with the FHp group (Table 2 and Fig. 2). The FHp group showed higher PiB retention than the FH− group in the MFG and PCC/precuneus, mostly of the left hemisphere (Table 2). No brain regions showed significantly higher PiB retention in the FH− group as compared
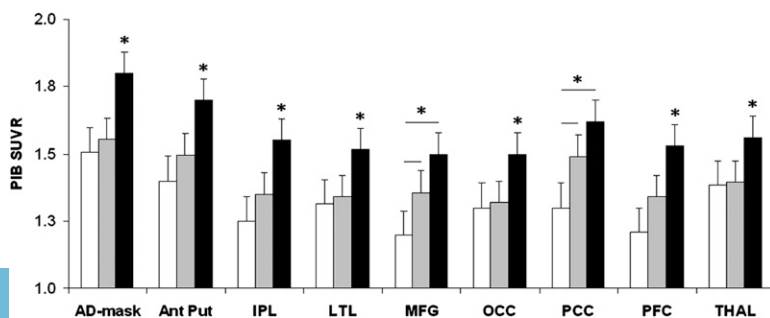

Fig. 1. Covariates-adjusted mean ROI PiB SUVR by family history group. Error bars are SEM. Asterisks mark significant differences at $P < 0.05$. Lines mark linear trends. White bars, FH−; gray bars, FHp; black bars, FHm. AntPut, anterior putamen, IPL, inferior parietal lobe; LTL, lateral temporal lobe; MFG, medial frontal gyrus; OCC, occipital cortex; PCC, posterior cingulate cortex/precuneus; PFC, prefrontal cortex; THAL, thalamus.

Mosconi et al.

Table 2. Brain regions showing significant differences in PiB retention across family history groups

Cluster extent	Coordinates (x, y, z)*	Z†	Functional area	Brodmann area
Higher PiB retention in FHm than in FHn				
850	−4 −54 16	3.85	Posterior cingulate cortex	23
	4 −59 12	3.46	Posterior cingulate cortex	30
	−3 −47 26	3.32	Posterior cingulate cortex	31
1339	−55 6 20	3.81	Inferior frontal gyrus	44
	−6 22 −21	3.75	Inferior frontal/rectal gyrus	11
	−47 11 32	3.66	Middle frontal gyrus	9
638	3 −59 12	3.77	Posterior cingulate gyrus	23/30
1236	−61 −18 4	3.65	Superior temporal gyrus	22
	−46 −51 −12	3.59	Fusiform gyrus	37
	−56 −34 5	3.40	Middle temporal gyrus	22
797	−55 −64 −4	3.62	Middle occipital gyrus	19
884	42 44 20	3.60	Middle frontal gyrus	10
	35 46 28	3.59	Superior frontal gyrus	9
248	−43 −37 45	3.52	Inferior parietal lobule	40
455	56 22 16	3.42	Inferior frontal gyrus	45
135	−7 60 4	3.40	Medial frontal gyrus	10
200	65 −30 6	3.37	Superior temporal gyrus	22
152	4 58 0	3.33	Medial frontal gyrus	10
209	−59 −59 24	3.29	Angular gyrus	39/40
218	53 −50 −16	3.33	Fusiform gyrus	37
208	51 −42 50	3.32	Inferior parietal lobule	40
131	−56 −33 45	3.29	Inferior parietal lobule	40
145	44 20 35	3.28	Middle frontal gyrus	9
119	−30 13 −16	3.24	Inferior frontal gyrus	47
86	−4 36 24	3.22	Anterior cingulate cortex	24
178	5 8 −1	3.20	Caudate	
	11 2 −4	3.18	Thalamus	
Higher PiB retention in FHm than in FHp				
1377	−8 −62 35	3.42	Precuneus	7
	6 −67 40	3.03	Precuneus	7
228	−3 −54 16	3.15	Posterior cingulate cortex	30
615	55 −62 -3	3.11	Middle occipital gyrus	37
421	−48 25 1	3.06	Inferior frontal gyrus	45
1113	4 25 20	3.05	Anterior cingulate cortex	24
	4 59 2	3.00	Medial frontal gyrus	10
420	−43 −37 45	3.02	Inferior parietal lobule	40
186	48 25 1	2.99	Inferior frontal gyrus	45
760	52 −41 50	2.98	Inferior parietal lobule	40
333	−65 −39 10	2.97	Superior temporal gyrus	22
141	−63 −39 -1	2.97	Middle temporal gyrus	21
275	12 2 16	2.99	Caudate	
Higher PiB retention in FHp than in FHn				
210	−3 −29 45	3.32	Precuneus	7
	−2 −39 35	3.07	Cingulate cortex	31
142	−3 54 20	3.18	Medial frontal gyrus	9

*Coordinates from Talairach and Tournoux.
†Z values at the peak of maximum significance at $P < 0.001$, uncorrected.

with the FHm or FHp groups or in the FHp group as compared with the FHm group. Results remained significant after accounting for age, education, gender, and ApoE status. Overall, PiB retention was higher in all brain regions in the FHm group than in the FHp and FH− groups. PiB retention in PCC and MFG was highest in the FHm group, intermediate in the FHp group, and lowest in the FH− group. This effect is illustrated in Fig. 3.

On logistic regression, all significant regions from the above analyses discriminated the FHm group from the FH− group and from the FHp group with accuracy between 68% and 82% ($P \leq 0.006$). The regions yielding the most accurate discrimination were the PCC for the FHm group vs. the FH− group [82% accuracy, 86% sensitivity, and 79% specificity, relative risk (RR) = 5.2 , 95% confidence interval (CI) = 1.9–16.9], and the parietal cortex for the FHm group vs. the FHp group (79% accuracy, 86% sensitivity, and 71% specificity, RR = 4.5, CI = 1.6–15.5). PiB retention in PCC was the only significant regional discriminator of the FHp group vs. the

FH− group, with 75% accuracy ([71% sensitivity and 79% specificity, RR = 3.2, CI = 1.3–8.3, $P = 0.001$).

Discussion

This study shows that NL individuals with a parent affected by LOAD have increased PiB retention, reflecting higher Aβ burden, in brain regions typically affected in clinical AD patients as compared with NL individuals with no family history. Additionally, we found significant parent-of-origin effects on Aβ deposition, with the FHm subjects showing increased and more widespread PiB retention than the FHp subjects.

Most neuropathological research in AD has provided evidence for a long, preclinical phase during which Aβ pathology accumulates in the brain of aging individuals for years before onset of clinical symptoms (4, 5). In vivo PiB-PET studies in AD patients demonstrated a pattern of tracer retention consistent with the known distribution of Aβ plaques observed at postmortem (6, 8, 9, 13, 14). A similar pattern was observed in many patients with mild
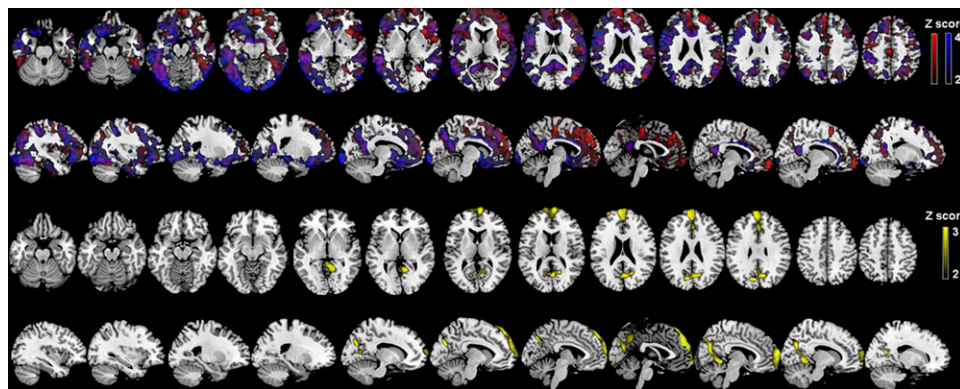
www.manaraa.com

MEDICAL SCIENCES

Fig. 2. SPMs showing higher PiB retention in NL FHm subjects than in FH− and FHp subjects (*Top Two Rows*) and in NL FHp subjects than in FH− subjects (*Bottom Two Rows*), as listed in Table 2. Areas of hypometabolism are represented on a red (FHm > FH−), blue (FHm > FHp), and yellow (FHp > FH−) color-coded scale, reflecting Z scores between 2 and 4. SPMs are displayed on the axial and sagittal views of a standard, spatially normalized MRI.

cognitive impairment and in elderly NL individuals (7–9, 13–15). Longitudinal studies in mild cognitive impairment have shown that increased PiB retention is predictive of future conversion to AD (16–18). Moreover, a recent study showed that PiB retention in NL subjects correlates with ApoE ε4 gene dose, a major genetic risk factor for AD (19). Our results report an association between Aβ load and a parental history of LOAD among NL individuals that may reflect increased predisposition for AD.

Although the genetic mechanisms involved in familial LOAD remain largely unknown, many studies have shown that Aβ accumulation is an early, initiating event in EOAD (1). PiB-PET studies showed that Aβ load was highest in the striatum of presymptomatic individuals carrying autosomal dominant mutations in the presenilin 1 and amyloid precursor protein genes (20, 21). The present study shows that Aβ deposition is more prominent in the cortical than in the subcortical regions in NL FH+ individuals at risk for

LOAD. This observation supports the idea that different patterns of Aβ deposition are associated with EOAD and LOAD (1, 20).

We observed differential effects of FH status on regional Aβ deposition. Although both the FHm and FHp groups showed increased PiB retention in the PCC and MFG as compared with controls, only the FHm group showed PiB retention in lateral neocortex. Braak's (4) pathologic studies showed that deposition of amyloid plaques begins in the inferior frontal and temporal cortex and spreads to adjacent PCC and medial frontal regions and then to the lateral parietal, prefrontal, and temporal regions (4). According to this postmortem staging, our NL FHm subjects appear to be at a more advanced stage of brain amyloidosis than the FHp subjects. Moreover, in the regions showing PiB retention for both the FHm and the FHp groups, Aβ burden was higher in FHm than in FHp subjects, suggesting a quantitative as well as topographical progression. Longitudinal studies mapping the spreading of fibrillar Aβ deposits are needed to determine whether FHm subjects develop amyloidosis at an earlier age than FHp subjects or show faster Aβ accumulation after middle age.

We and others previously have shown a reduced cerebral metabolic rate for glucose consumption (CMRglc) on FDG-PET (10, 11), reduced blood oxygen level-dependent signal on functional MRI (22), and reduced gray matter (GM) volumes on MRI (12) in the NL FH+ group as compared with the FH− group, as well as more severe deficits in the NL FHm group than in the FHp group (10–12). Similar abnormalities were shown to be predictive of decline from normal cognition to dementia (23–25). However, FDG-PET and MRI measures are surrogate markers of AD, most likely reflecting the functional and structural consequences of other pathognomonic mechanisms, and doubt remained as to whether the brain changes observed in prior studies were the result of AD pathology or other causes. Present PiB-PET findings show that Aβ pathology may account, at least in part, for the previously observed abnormalities. Collectively, our PiB and FDG-PET studies (10, 11) show that NL FHm subjects in their early 60s have significant reductions in CMRglc and increased Aβ load in AD regions, whereas NL FHp subjects of the same age range have some Aβ deposits in the absence of hypometabolism. These data suggest that amyloidosis may precede neuronal dysfunction in FHp subjects. On the other hand, the presence of both Aβ pathology and hypometabolism in middle-aged to old NL FHm subjects indicates that these brain abnormalities developed at younger ages in these subjects. The temporal and causal relationship between Aβ and glucose dysmetabolism in AD remains to be established. Nonetheless, with all that is known about the mechanisms involved in glucose utilization and maternal inheritance, evidence for early oxidative dysmetabolism in the FHm group suggests transmission through mitochondrial genes, which are entirely maternally inherited in humans (26) and whose expression is known to affect Aβ production in AD (27). CMRglc abnormalities in NL FHm subjects
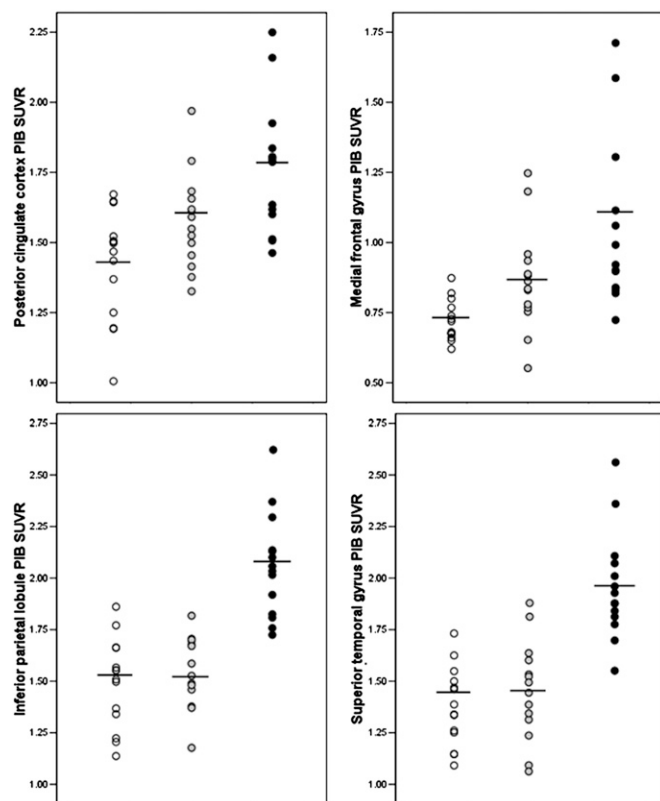

Fig. 3. PiB SUVR measures extracted from the clusters showing maximal statistical differences across NL FHm subjects (black circles), FHp subjects (gray circles), and FH− subjects (open circles), as listed in Table 2.

Mosconi et al.

www.manaraa.com

may be an early, maternally inherited abnormality that increases vulnerability to Aβ pathology during the aging process. Alternatively, CMRglc abnormalities may be secondary to the toxic effects of Aβ (1). Mitochondria are major intracellular targets of soluble Aβ oligomers, which cause overproduction of reactive oxygen species, disrupt intracellular calcium homeostasis, and trigger neuronal apoptosis (27). Although Aβ oligomers are not detectable with PiB-PET, prolonged production of oligomers eventually would result in the formation of fibrils. Aβ plaques, in turn, often are surrounded by microglia and astrocytes, a major source of mitochondrial oxidative stress (26).

Present findings of higher risk in NL FHm individuals than in FHp individuals are consistent with epidemiology studies showing an important role for maternal transmission in LOAD. Although there is mixed evidence for parent-gender effects in LOAD (28, 29), maternal transmission is more frequent than paternal transmission and is associated with poorer cognitive performance in late life and with a more predictable age at onset of dementia (28, 30–32). Our findings of more prominent Aβ abnormalities and associated AD risk in FHm than in FHp subjects are consistent with epidemiological findings and provide a possible pathophysiological substrate to the clinical data.

Steps were taken to ensure that the AD diagnosis in the subjects' parents was accurate. We included only subjects whose parents' AD diagnosis was clinician certified, and FH questionnaires are known to have good agreement with clinical and neuropathological findings (33). Nonetheless, our cohort may have included subjects whose parents did not have AD but instead had another dementia. The inclusion of such subjects could reduce power in detecting group differences. Examination of the four individuals whose parents had postmortem-confirmed AD supports the observation of more prominent Aβ deposition in FHm subjects than in FHp subjects. However, additional phenotypic effects in FHp subjects may not have been detected because of the relatively small sample and conservative statistical procedures. Replication studies with larger samples are warranted to examine this question.

The finding of different levels of Aβ load in relation to FH status resembles observations in NL carriers of different copies of the ApoE ε4 allele (19). Although the genetic factors involved in our findings are not known, present results were independent of ApoE genotype and were significant within the ApoE ε4+ group. Moreover, none of our FHm subjects were ε4/ε4 carriers. Nonetheless, a relatively high proportion of our FH+ subjects were ApoE ε4+, probably because the ApoE ε4 genotype is overrepresented in LOAD (2) and because FH+ individuals are more likely to worry about their cognitive status and seek clinical attention. Therefore, the frequency of ApoE ε4+ often is higher in the "worried-well" subjects who self-refer to memory clinics and associated research settings such as ours. Studies are needed to examine the interactions between FH and ApoE status on brain amyloidosis and to replicate present research findings in community-based samples.

Previous studies examined PiB measures as dichotomous or continuous variables. Only a minority of our NL subjects could be classified as PiB+, including one FH− subject, one FHp subject, and two FHm subjects. Therefore, the frequency of PiB+ scans was not different across FH groups. Conversely, by treating PiB as a continuous variable, we observed quantitative differences across FH groups that included so-called "PiB−" subjects. Our findings are consistent with previous studies showing that PiB signal is distributed continuously among elderly NL individuals and is sensitive enough to detect abnormalities in individuals with apparently minimal pathology (15, 19, 34).

NL FHm subjects showed increased PiB binding in the occipital cortex in addition to the parietotemporal, PCC, and frontal regions. This observation is consistent with previous reports of occipital PiB retention in AD and NL ApoE ε4 carriers (6, 19), which may be caused mainly by tracer binding to cerebrovascular

Aβ (i.e., cerebral amyloid angiopathy) (35). Our data indicate that NL FHm subjects present with both parenchymal and vascular Aβ deposits, findings that often co-occur in AD (35).

Because the definitive diagnosis of AD is based on presence of Aβ plaques and neurofibrillary tangles (NFT), studies are needed to examine tau pathology in NL FH+ subjects. At present, NFT imaging is under development. Among available PET tracers, 2-(1-96-(2-^{18}F-fluoroethyl)(methyl)amino)-2-naphthyl)ethyldene) malono nitrile (^{18}F-FDDNP) binds to both Aβ fibrils and NFT and shows longitudinal progression in nondemented individuals (36). Converging information from multiple markers of AD pathology is desirable for a specific, early diagnosis of AD.

In conclusion, the present PiB-PET study shows increased fibrillar Aβ in NL persons with a parental history of LOAD, particularly in persons with an AD mother. These findings may motivate further research on parent-of-origin effects at the presymptomatic stages of AD. Detection of brain Aβ in NL FH+ subjects represents a unique opportunity for initiation of AD therapies and general preventive methods years, and possibly decades, before the onset of clinical disease.

Materials and Methods

Subjects. This study examines a cohort of 42 consecutive NL individuals from our longitudinal studies at New York University (NYU) and at the University of Turku, Finland, divided into three groups of 14 subjects each: NL individuals with an AD mother, NL individuals with an AD father, and NL individuals without a FH of AD. Subjects were previously derived from multiple community sources, including individuals interested in research participation and family members and caregivers of impaired patients (10, 14). All subjects provided written informed consent to participate in this Internal Review Board-approved study and received thorough clinical and neuropsychological examinations and MRI and PiB-PET scans.

Individuals with medical conditions or history of significant conditions that might affect brain structure or function (i.e., stroke, diabetes, head trauma, any neurodegenerative diseases, depression, MRI evidence of hydrocephalus, intracranial mass, and infarcts including lacunes) and those taking psychoactive medications were excluded. Subjects were 50–80 years of age, had a Clinical Dementia Rating of 0, Global Deterioration Scale ≤2, Modified Hachinski Ischemia Scale score <4, Geriatric Depression Scale score ≤5, MMSE score ≥26, and normal cognitive test performance relative to appropriate normative values for age and education (10, 14). ApoE genotype was determined using standard PCR procedures.

A FH that included at least one first-degree relative whose AD onset was between age 60 and 80 years was elicited by using a standardized FH questionnaire (11). Participants filled in demographical and clinical information for all affected family members over three generations. The information was confirmed with other family members in the interview with the examining neurologist. Subjects were included only if their parents had lived to age 60 years, and parents' diagnosis had been made by a certified clinician according to established criteria for AD (35). Only NL FH+ individuals were examined and were compared with NL individuals with a FH negative for any dementia (FH−). The AD-affected parents of two FHm individuals and two FHp individuals had received an autopsy-confirmed postmortem diagnosis of AD.

Brain Imaging. All subjects received standardized, whole-brain clinical T2-weighted and research 3D T1-weighted MRI protocols at 1.5 T (NYU: General Electric Signa imager; Turku: Philips CV Nova Dual scanner), and a PET scan with N-methyl[^{11}C]2-(4'-methylaminophenyl)-6-hydroxy-benzothiazole (PiB) as the tracer. PiB was synthesized on site from the reaction of 6-OH-BTA-0 and [^{11}C]methyl triflate. Radiochemical purity of the radioligand was >98%. Before PET imaging, an antecubital venous line was positioned for isotope injection. Subjects were rested with eyes open and ears unplugged in the quiet and dimly lit scan room. After injection of 15 mCi (~550 MBq) of PiB, subjects were positioned in the scanner using laser light beams for head alignment. At both centers, scans were acquired in 3D mode on a General Electric PET scanner (NYU: LS Discovery, Turku: GE Advance). Total scanning time was 90 min. No blood sampling was performed. All images were corrected for photon attenuation, scatter, and radioactive decay and were reconstructed into a 128 × 128 matrix spaced every 4.25 mm.

Image processing and data analyses were performed at NYU blind to clinical information. Summed PET images corresponding to the 60–90 min of PiB data were created for both data sets and were coregistered to T1-MRI using a surface-fitting algorithm implemented in MIDAS 1.9 (15). Standardized uptake values (SUV) were determined on a voxel-wise basis (37). A

Mosconi et al.

www.manaraa.com

MEDICAL SCIENCES

cerebellar GM region was delineated on MRI and used as the reference to correct (normalize) for nonspecific tracer binding (38) by dividing each voxel's SUV into the cerebellar SUV, yielding parametric PiB SUV ratio (SUVR) images. This procedure was shown to yield PiB estimates equivalent to compartmental modeling (37, 39). Parametric PiB SUVR images were processed using SPM5 (40) and automated ROI (14, 15). Briefly, subjects' MRIs were normalized spatially to a standardized MRI brain template image, which approximates the Talairach and Tournoux space, by estimating the optimum least-squares, 12-parameter affine transformation, followed by $7 \times 8 \times 7$ cosine functions. These parameters were applied to MRI-coregistered PiB scans to generate spatially normalized PiB SUVR images. Automated ROIs were used to sample GM within AD-related brain regions, including the anterior putamen, IPL, LTL, medial frontal gyrus, PCC/precuneus, PFC, OCC, and thalamus (15). A cortical PiB retention mask (AD-mask) also was created by combining the cortical ROIs. For each subject, an inverse polynomial transformation was applied to the ROIs in the template space to warp the atlas to the subject's native anatomical space (15).

Spatially normalized PiB images then were smoothed with a 12-mm Gaussian filter and were examined for voxel-wise effects across groups (14). As a result of the cerebellar normalization of PiB data, no proportional scaling or grand mean scaling was performed. A GM mask was generated from the SPM5 a priori GM template by retaining voxels with values ≥ 0.8 (i.e., the probability of the voxel's contents being GM was $\geq 80\%$) and was included as an explicit mask to perform group comparisons exclusively within GM voxels. Only clusters of 30 or more voxels were considered significant.

Statistical Analysis. Analyses were done with SPSS 12.0 and SPM5. Differences in clinical and ROI measures between FH groups were examined with the General Linear Model (GLM) with posthoc Least Significant Difference tests and χ^2 tests. FH status was dummy coded using two variables, FH status (FH− vs. FH+) and parent gender (FH− vs. FHp vs. FHm). Results were examined at

$P < 0.05$. For SPM5 analysis, the GLM was used to test for regional differences in parametric PiB SUVR images across FH groups. Main group effects were examined using F contrasts, followed with post hoc T-contrasts to test for pair-wise intergroup comparisons. Results were examined at $P < 0.001$, uncorrected for multiple comparisons. The GLM was used to examine the effects on PiB of other possible risk factors for LOAD, such as age, gender, education, and ApoE genotype. Before analysis, we examined scanner type for effects on PiB using the GLM and found no significant effects in any ROIs ($P \geq 1$). Anatomical location of brain regions showing significant effects was described using Talairach and Tournoux coordinates, after conversion from the Montreal Neurological Institute (MNI) to the Talairach space using linear transformations (http://www.mrc-cbu.cam.ac.uk/Imaging/).

Because ApoE ε4 genotype is associated with LOAD, we examined the effects of FH status on PiB within the group of ApoE ε4+ subjects using nonparametric Mann–Whitney rank sum tests (α = 0.05, exact significance, one-tailed).

PiB SUVR scans of the subjects with pathology-verified AD parents were Z scored relative to FH− subjects, and Z scores ≥1.5 SD from controls were considered significant.

Stepwise forward logistic regressions with χ^2 tests were used to determine sensitivity, specificity, accuracy, and relative risk of regional PiB measures as predictors of group membership (FH− vs. FHm vs. FHp) and to identify the most significant regional predictor for each contrast, after controlling for age, gender, education, and ApoE genotype ($P < 0.05$).

1. Hardy J, Selkoe DJ (2002) The amyloid hypothesis of Alzheimer's disease: Progress and problems on the road to therapeutics. *Science* 297:353–356.
2. Farrer LA, et al.; APOE and Alzheimer Disease Meta Analysis Consortium (1997) Effects of age, sex, and ethnicity on the association between apolipoprotein E genotype and Alzheimer disease. A meta-analysis. *JAMA* 278:1349–1356.
3. Green RC, et al.; MIRAGE Study Group (2002) Risk of dementia among white and African American relatives of patients with Alzheimer disease. *JAMA* 287:329–336.
4. Braak H, Braak E (1991) Neuropathological staging of Alzheimer-related changes. *Acta Neuropathol* 82:239–259.
5. Price JL, Morris JC (1999) Tangles and plaques in nondemented aging and "preclinical" Alzheimer's disease. *Ann Neurol* 45:358–368.
6. Klunk WE, et al. (2004) Imaging brain amyloid in Alzheimer's disease with Pittsburgh Compound-B. *Ann Neurol* 55:306–319.
7. Kemppainen NM, et al. (2007) PET amyloid ligand [^{11}C]PIB uptake is increased in mild cognitive impairment. *Neurology* 68:1603–1606.
8. Pike KE, et al. (2007) Beta-amyloid imaging and memory in non-demented individuals: Evidence for preclinical Alzheimer's disease. *Brain* 130:2837–2844.
9. Mintun M, et al. (2006) [^{11}C]PIB in a nondemented population: Potential antecedent marker of Alzheimer's disease. *Neurology* 67:446–452.
10. Mosconi L, et al. (2007) Maternal family history of Alzheimer's disease predisposes to reduced brain glucose metabolism. *Proc Natl Acad Sci USA* 48:19067–19072.
11. Mosconi L, et al. (2009) Declining brain glucose metabolism in normal individuals with a maternal history of Alzheimer's. *Neurology* 72:513–520.
12. Honea RA, Swerdlow RH, Vidoni E, Goodwin J, Burns JM (2010) Reduced gray matter volume in normal adults with a maternal family history of Alzheimer disease. *Neurology* 74:113–120.
13. Rowe CC, et al. (2007) Imaging {beta}-amyloid burden in aging and dementia. *Neurology* 68:1718–1725.
14. Kemppainen N, et al. (2006) Voxel-based analysis of PET amyloid ligand [^{11}C]PIB uptake in Alzheimer disease. *Neurology* 67:1575–1580.
15. Li Y, et al. (2008) Regional analysis of FDG and PIB-PET images in normal aging, mild cognitive impairment, and Alzheimer's disease. *Eur J Nucl Med Mol Imaging* 35:2169–2181.
16. Forsberg A, et al. (2008) PET imaging of amyloid deposition in patients with mild cognitive impairment. *Neurobiol Aging* 29:1456–1465.
17. Okello A, et al. (2009) Conversion of amyloid positive and negative MCI to AD over 3 years. An ^{11}C-PIB PET study. *Neurology*, in press.
18. Wolk DA, et al. (2009) Amyloid imaging in mild cognitive impairment subtypes. *Ann Neurol* 65:557–568.
19. Reiman EM, et al. (2009) Fibrillar amyloid-beta burden in cognitively normal people at 3 levels of genetic risk for Alzheimer's disease. *Proc Natl Acad Sci USA* 106:6820–6825.
20. Klunk WE, et al. (2007) Amyloid deposition begins in the striatum of presenilin-1 mutation carriers from two unrelated pedigrees. *J Neurosci* 27:6174–6184.
21. Remes AM, et al. (2008) Carbon 11-labeled Pittsburgh compound B positron emission tomographic amyloid imaging in patients with APP locus duplication. *Arch Neurol* 65:540–544.
22. Johnson SC, et al. (2006) The influence of Alzheimer disease family history and apolipoprotein E epsilon4 on mesial temporal lobe activation. *J Neurosci* 26:6069–6076.
23. de Leon MJ, et al. (2001) Prediction of cognitive decline in normal elderly subjects with 2-[(18)F]fluoro-2-deoxy-D-glucose/positron-emission tomography (FDG/PET). *Proc Natl Acad Sci USA* 98:10966–10971.
24. Jack CR, Jr, et al. (2005) Brain atrophy rates predict subsequent clinical conversion in normal elderly and amnestic MCI. *Neurology* 65:1227–1231.
25. Mosconi L, et al. (2008) Hippocampal hypometabolism predicts cognitive decline from normal aging. *Neurobiol Aging* 29:676–692.
26. Lin MT, Beal MF (2006) Mitochondrial dysfunction and oxidative stress in neurodegenerative diseases. *Nature* 443:787–795.
27. Green KN, LaFerla FM (2008) Linking calcium to Abeta and Alzheimer's disease. *Neuron* 59:190–194.
28. Edland SD, et al. (1996) Increased risk of dementia in mothers of Alzheimer's disease cases: Evidence for maternal inheritance. *Neurology* 47:254–256.
29. Ehrenkrantz D, et al. (1999) Genetic epidemiological study of maternal and paternal transmission of Alzheimer's disease. *Am J Med Genet* 88:378–382.
30. Gómez-Tortosa E, et al. (2007) Variability of age at onset in siblings with familial Alzheimer disease. *Arch Neurol* 64:1743–1748.
31. Silverman JM, Ciresi G, Smith CJ, Marin DB, Schnaider-Beeri M (2005) Variability of familial risk of Alzheimer disease across the late life span. *Arch Gen Psychiatry* 62:565–573.
32. Debette S, et al. (2009) Association of parental dementia with cognitive and brain MRI measures in middle-aged adults. *Neurology* 73:2071–2078.
33. Kawas C, Segal J, Stewart WF, Corrada M, Thal LJ (1994) A validation study of the Dementia Questionnaire. *Arch Neurol* 51:901–906.
34. Mormino EC, et al.; Alzheimer's Disease Neuroimaging Initiative (2009) Episodic memory loss is related to hippocampal-mediated beta-amyloid deposition in elderly subjects. *Brain* 132:1310–1323.
35. Johnson KA, et al. (2007) Imaging of amyloid burden and distribution in cerebral amyloid angiopathy. *Ann Neurol* 62:229–234.
36. Small GW, et al. (2006) PET of brain amyloid and tau in mild cognitive impairment. *N Engl J Med* 355:2652–2663.
37. Price JC, et al. (2005) Kinetic modeling of amyloid binding in humans using PET imaging and Pittsburgh Compound-B. *J Cereb Blood Flow Metab* 25:1528–1547.
38. McKhann G, et al. (1984) Clinical diagnosis of Alzheimer's disease: Report of the NINCDS-ADRDA Work Group under the auspices of Department of Health and Human Services Task Force on Alzheimer's Disease. *Neurology* 34:939–944.
39. Lopresti BJ, et al. (2005) Simplified quantification of Pittsburgh Compound B amyloid imaging PET studies: A comparative analysis. *J Nucl Med* 46:1959–1972.
40. Friston KJ, et al. (1995) Statistical parametric maps in functional imaging: A general linear approach. *Hum Brain Mapp* 2:189–210.

www.manaraa.com